Electrochimica Acta 446 (2023) 142009

Contents lists available at ScienceDirect

Electrochimica Acta

journal homepage: www.journals.elsevier.com/electrochimica-acta

Integration of smart nanomaterials for highly selective disposable sensors and their forensic applications in amphetamine determination

Meshal H. Almabadi [a], Florina Maria Truta [b], Gyako Adamu [a], Todd Cowen [a], Mihaela Tertis [b], Ana-Maria Drăgan [b], Kaseb D.M. Alanazi [a], Maria-Georgia Ștefan [c], Elena Piletska [a], Béla Kiss [c], Cecilia Cristea [b], Karolien De Wael [d], Sergey A. Piletsky [a], Alvaro Garcia Cruz [a,*]

[a] Biotechnology Group, Department of Chemistry, University of Leicester, United Kingdom
[b] Department of Analytical Chemistry, Faculty of Pharmacy, Iuliu Haţieganu University of Medicine and Pharmacy, 4 Pasteur Street, Cluj-Napoca 400349, Romania
[c] Department of Toxicology, Faculty of Pharmacy, Iuliu Haţieganu University of Medicine and Pharmacy, 8 Victor Babes, Cluj-Napoca 400012, Romania
[d] Department of Bioscience Engineering, University of Antwerp, Belgium. Groenenborgerlaan 171, Antwerp B-2020, Belgium

ARTICLE INFO

Keywords:
Molecularly imprinted polymer
Nanoparticles
Electrochemical sensor
Forensics
Amphetamine

ABSTRACT

Screening drugs on the street and biological samples pose a challenge to law enforcement agencies due to existing detection methods and instrument limitations. Herein we present a graphene-assisted molecularly imprinted polymer nanoparticle-based sensor for amphetamine. These nanoparticles are electroactive by incorporating ferrocene in their structure. These particles act as specific actuators in electrochemical sensors, and the presence of a ferrocene redox probe embedded in the structure allows the detection of non-electroactive amphetamine. In a control approach, nanoparticles were covalently immobilised onto electrochemical sensors by drop-casting using silanes. Alternatively, nanoparticles were immobilised employing 3D printing and a graphene ink composite. The electrochemical performance of both approaches was evaluated. As a result, 3D printed nanoMIPs/graphene sensors displayed the highest selectivity in spiked human plasma, with sensitivity at 73 nA nM^{-1}, LOD of 68 nM (RSD 2.4%) when compared to the silane drop cast electrodes. The main advantage of the optimised 3D printing technology is that it allows quantitative determination of amphetamine, a non-electroactive drug, challenging to detect with conventional electrochemical sensors. In addition, the cost-efficient 3D printing method makes these sensors easy to manufacture, leading to robust, highly selective and sensitive sensors. As proof of concept, sensors were evaluated on the street specimens and clinically relevant samples and successfully validated using UPLC-MS.

1. Introduction

Amphetamine is a potent central nervous system stimulant used to treat several diseases, including attention deficit hyperactivity disorder, anxiety, narcolepsy, depression, and other psychological disorders [1–3]. Due to its importance in medical applications, the administration of amphetamine needs to be monitored for side effects, such as high blood pressure, anorexia, blurred vision, etc. The constant administration of amphetamine can itself cause anxiety disorders, insomnia and mood swings [4]. The determination of amphetamine is also critical for forensic control. The United Nations Office on Drugs and Crime (UNODC) ranks amphetamine-type stimulants as the world's second most widely seized class of drug after cannabis [5]. Amphetamine and illicit drugs require quantitative techniques applicable in solids and biological samples. Therefore, there is a need for a flexible, low-cost, portable, and accurate device for drug detection.

Amphetamine is typically prescribed as a medicinal drug in single doses, of approximately 5–10 mg, resulting in a blood concentration of 148 to 220 nM (20–30 ng mL^{-1}). Doses exceeding 30 mg (0.10–0.15 ng L^{-1}, 700–1100 nM) are not recommended, and higher blood concentrations (1480 nM) may be toxic. Screening for amphetamine is usually performed with an immunological test with a cut-off at 0.05 mg L^{-1} (0.4

Abbreviations: MIP, Molecularly Imprinted Polymers; nanoMIPs, Molecularly Imprinted Polymer Nanoparticles; UHPLC, Ultra-high Performance Liquid-Chromatography; MOE, Molecular Operating Environment; DLS, Dynamic Light Scattering; EDX, Energy-DispersiveX-rayspectroscopy; SEM, Scanning Electron Microscopy; TEM, Transmission Electron Microscopy; SPPE, Screen-Printed Platinum Electrodes; LOD, Limit of Detection.

* Corresponding author.
E-mail address: agc14@leicester.ac.uk (A. Garcia Cruz).

https://doi.org/10.1016/j.electacta.2023.142009
Received 15 August 2022; Received in revised form 17 January 2023; Accepted 3 February 2023
Available online 9 February 2023

μM) [6] and by gas chromatography-mass spectrometry (GC–MS) with a cut off at 0.04 mg L^{-1} (0.3 μM) [7,8] However, these methods have several drawbacks, including lengthy sample preparation, expensive laboratory-based techniques, specialized instrumentation and qualified personnel.

Alternately, they are available several colorimetric tests [9] and portable spectrometric devices (Near infrared [10], Raman [11] and mass spectroscopy [12] technology) for border control. Unfortunately, these technologies are challenging to apply for rapid drug screening without avoiding false negatives in samples with high chemical complexity in the presence of biological matrixes and different cutting agents. For this reason, they present cross-reactivity and insufficient selectivity. Even all the available analytical screening techniques, accurate drug checking and the quantification of compounds are still limited [13]. There is therefore a huge demand from law enforcement agencies for new technologies that can facilitate the screening of street samples [14].

Electrochemical sensors have recently been used for drug detection in biological and seized samples [15,16]. The critical advantages of an electrochemical sensor are their portability, accuracy, and low cost [17]. Classic electrochemical sensors are used to determine the direct electro-oxidation of the analyte [18,19]. Unfortunately, direct electro-oxidation of the analyte may lack of selectivity and produces side reactions. This technique also cannot be applied for amphetamine determination due to the absence of analyte electroactivity [19]. Electro-oxidation becomes particularly inaccurate when these sensors are applied to biological fluids, due to false positives from interferences, endogenous electroactive molecules and the inherent matrix effect. Traditional biosensors have been employed to overcome those challenges [20,21]. Regrettably, they require a specific enzyme or antibody for their functioning, limiting their commercial applications due to their fragile nature and challenging integration process in sensors.

An alternative approach is to use synthetic receptors known as molecularly imprinted polymers (MIPs) [19,22]. MIPs are advantageous for their polymeric nature, ease of synthesis, resistance to harsh conditions (pH, temperature etc.) and long shelf-life [17,23]. The MIP sensor approaches frequently use membranes and micro microspheres polymers as recognition elements [17,24,25]. Commonly, these sensors use the electro-oxidation of the analyte or a redox probe in solution to generate the sensor signal, limiting their application in biological samples due to side reactions and interferences present in the sample [22, 26]. Recent research on MIP electrochemical sensors uses the combination of ferrocene and nanostructured carbon material, giving improvements in conductivity and sensitivity and easy adaption to manufacturing using printing techniques [27–30]. Nevertheless, on these sensors, MIPs are porous permeable membranes deposited as film composites [29,31,32]. In this case, the analyte binding causes a structural MIP polymer arrangement by swelling or shrinking. This can lead to a charge accumulation modifying the diffusion rate of electrolyte ions or/and the redox probe through the film known as gate effect [26,28].

The present technology represents an improvement of the existing MIP-based sensors (e.g. membranes, microspheres or monolithic MIPs) due to their selective nanoscale actuation combined with electroactivity provided by the presence of ferrocene in the polymer matrix. Therefore, the key advantages of using nanoMIP over common MIP films based sensors are the improvement in sensitivity and selectivity. From a manufacturing perspective, nanoMIP allows the easily large-scale production through automated reactors [33], which increases their reproducibility and, secondly, the compatibility with different integration methods such as printing [34,35]. NanoMIPs are highly selective and sensitive, capable of mimicking the specificity of natural receptors, which makes them suitable for the analysis of biological samples [19, 36]. NanoMIP play the role of both recognition and reporting components that increase the selectivity and sensitivity of sensors [37–39]. For this reason, nanoMIPs have been used to replace enzyme-mediator pairs used in traditional biosensors and antibodies in microplate assays [36, 40,41].

For all these advantages, several efforts have been made to integrate nanoMIP into sensors [17]. The commonly used electropolymerization and drop casting of MIP are not suitable methods for large-scale manufacturing. Therefore, different methods have been employed to integrate nanoMIP on sensors, such as binders and carbon composites, to be used for screen-printing [42]. Recently, nanoMIP have been integrated into sensors using cross-linkers such as mercaptans and silanes, and through immobilization in polymers [43–45]. In this work, we present two innovative approaches to integrate nanoMIPs particles via ink printing methods. The first approach uses direct drop-casting of nanoMIPs and covalent immobilization, and the second uses printing of a nanoMIP/graphene composite ink. The comparative performance of both approaches is analysed and the applicability in human samples and street samples was assessed.

2. Materials and methods

Amphetamine solution in methanol (Cerilliant, standard solution of 1 mg mL^{-1}), 3-aminopropyltrimethyloxysilane (APTES), N-(6-aminohexyl)aminomethyltriethoxysilane (AHAMTES), glutaraldehyde, 1,2-Bis (triethoxysilyl)ethane (BTSE), N-hydroxy-succinimide (NHS), Ferrocene methylmethacrylate (FcMMA), 2-Hydroxyethyl methacrylate (HEM), Itaconic acid (ITA), 1-ethyl-3-(3-dimethylaminopropyl)-carbodiimide hydrochloride (EDC), ethylene glycol dimethacrylate (EGDMA), trimethylolpropane trimethacrylate (TRIM), pentaerythritol tetrakis(3-mercaptopropionate) (PETMP), and sodium hydroxide (NaOH), were purchase from Sigma-Aldrich, UK. Phosphate buffered saline (PBS) consisted of phosphate buffer (0.01 M), potassium chloride (0.003 M), and sodium chloride (0.140 M), pH 7.4 was procured prom Gibco Life technologies Ltd, UK. Dimethylformamide (DMF), acetonitrile HPLC Grade and acetone were from Fisher Scientific, UK. The N,N-diethyldithiocarbamic acid benzyl ester was purchased from TCI Europe (Belgium) and used as initiator, transfer agent, and terminator (iniferter). Double-distilled ultrapure water (Millipore, UK) was used for the experiments. All chemicals and solvents were used without further purification. Lyophilized human plasma (S2257–5ML) was purchased from Sigma Aldrich.

The polymerization reaction was completed using UV sources (Philips HB/ 171 / A, 0.5 W cm^{-1},4 × 15 W lamps). Solid-phase extraction cartridges (SPE) with polyethylene frit (20 μm porosity, Supelco) were then used for the elution of nanoMIPs. For the polymer filtration and purification, disposable plastic syringes with cellulose acetate filter (25 mm, 0.45 μm, Whatman) and SnakeSkin dialysis tubes (Spectra/ Por 7, regenerated cellulose, reference 132,119, 10 kW MWCO, tube length 11 cm, flat width 32 mm, diameter 20.4 mm, 3.3 mL cm^{-1}) were employed. The electrochemical measurements were performed using screen printed platinum electrodes (SPPE, Dropsens DRP-550, Metrohm, UK) with dimensions of 3.4 × 1.0 × 0.05 cm (Length x Width x Height) and a three-electrode set-up (platinum working electrode, platinum counter electrode and silver reference electrode). A nitrogen plasma cleaner was used to activate the electrode surface (Emitech, K1050X RF Plasma Cleaner, 50 W, 13.56 MHz RF for 5 min). All the electrochemical measurements were performed by using a potentiostat/ galvanostat/ impedance analyser (PalmSens4 and EmstatBlue8) equipped with a cable connector for screen-printed electrodes. The PSTrace software (PalmSens, Netherlands) was employed to perform the experiments and for the data acquisition.

2.1. Molecular modelling

The polymer composition is first selcted through molecular modelling and screening of monomers [1–4]. Two approaches were used for the molecular modelling. The Sybyl modelling package was employed for monomer screening, and the Molecular Operating Environment (MOE) software was used to analyse specific interaction (Section 1,

Supporting information). The Leapfrog screening algorithm (as part of the Sybyl package) was used to select the most suitable functional monomers by measuring the propensity of each to bind to the target molecule. These were then verified using a screening method available with MOE. The structure of the target amphetamine was first optimized by energetic minimization to a 0.01 kcal mol^{-1} A^{-2} (0.04 kJ mol^{-1} A^{-2}) gradient using the default Tripos force field and an applied dielectric constant of 80 to simulate an aqueous environment. The geometry of each monomer, as present in the virtual library, had previously been minimised and refined using Tripos force fields with Gasteiger-Hückel charges to a gradient of 0.001 kcal mol^{-1} A^{-2} (0.004 kJ mol^{-1} A^{-2}).

The screening library contained 250 functional monomers commonly used in molecular imprinting, each of which possessed vinyl or allyl polymerizable moieties and functional groups suited to non-covalent interactions. The Sybyl Leapfrog screening algorithm is then initiated and set to 60,000 iterations. In this method a database of functional monomers are sequentially positioned around the target at specific interaction points. Each of these monomer-template interactions is then optimized by small movements of the monomer. These specific interactions between the monomer and the target are evaluated in terms of binding scores (kcal mol^{-1}), with the most promising candidates showing the greatest reduction in energy on monomer-template complexation.

The MOE screening method works on a similar basis to the Leapfrog screening, but with fewer automated assumption. In this screening, each monomer is analysed sequentially, being placed in 10 s or 100 s of copies randomly around the template. The results therefore represent an increase in accuracy over Sybyl, but at a greater computational expense and loss of efficiency. Replicating the results used in the Sybyl screening with MOE however, and adjustment to MMFF94 force field, the results were found to be consistent and converge at the same result. According to the screening of functional monomers, Itaconic acid "ITA" (−14.33 kcal mol^{-1}, −60 kJ) and Hydroxyethyl methacrylate "HEM" (−5.06 kcal mol^{-1}, −21.2 kJ) provide the highest binding to amphetamine, as shown in Fig. S1 (Section 1, Supporting information). The molecular modelling was performed by taking into account the tethered amphetamine to the solid phase (silane chain) as analyte in order to simulate the polymerization. According to the modelling, ITA and HEM are the best functional monomers that bind to amphetamine, and the optimum molecular ratio between amphetamine, ITA and HEM was found 1:1:1.

2.2. Synthesis of nanoMIPs

NanoMIPs monomer composition was computationally designed to recognise amphetamine and then synthesised by solid phase method. The synthesis process was summarized in Fig. 1, more details regarding the synthesis protocol are presented in (Section 2, Supporting information). The immobilization of amphetamine (template) was achieved by functionalizing the glass microspheres with cross-linkers, followed by covalent attachment of amphetamine, as shown in Fig. 1. Glass

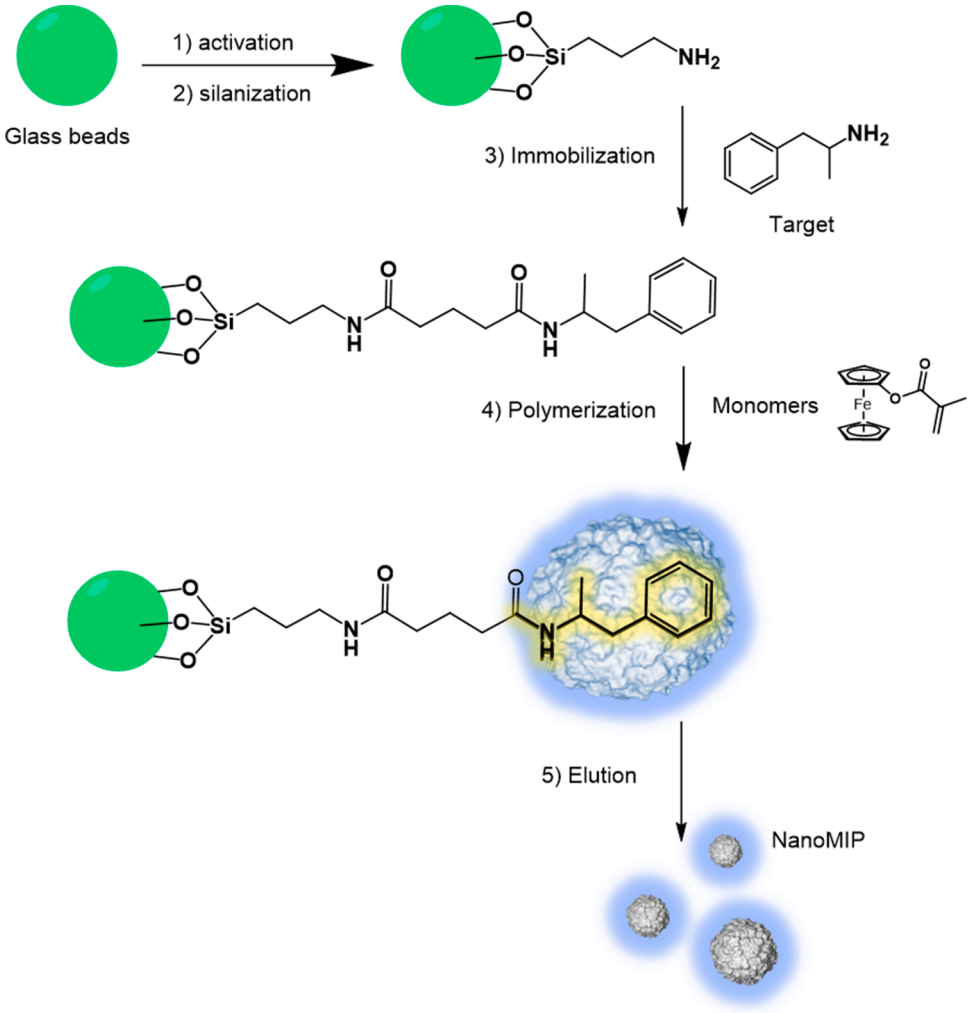

Fig. 1. Schematic representation of the experimental protocol applied for solid phase synthesis of the nanoMIPs specific for amphetamine. The process involve: (1) activation of the glass microspheres, (2) silanization and (3) immobilization of amphetamine on the solid phase, (4) polymerization and (5) elution of the nanoMIPs.

microspheres (30 g) were incubated in 40 mL of a solution of 7% (v/v) of glutaraldehyde in 5 mM PBS (pH 7.2) for 2 h. The glass microspheres were then rinsed with double-distilled water (100 mL) followed by incubation in an amphetamine solution (0.1 mg mL^{-1} in 5 mM PBS, pH 7.2) overnight at room temperature. The glass microspheres were then rinsed with double-distilled water (100 mL) and incubated in 50 mL of 0.1 mM ethanolamine in 5 mM PBS for 15 min. Subsequently, the glass microspheres were washed with distilled water and incubated in a 1 mg mL^{-1} sodium cyanoborohydride solution (in 5 mM PBS, 1.5 mL of solution per gram of microspheres) for 30 min at room temperature. Finally, the amphetamine modified glass microspheres were filtered and rinsed with ultrapure water, dried and stored at 4 °C until use (Table S1). For the nanoMIP synthesis, 2.18 g ITA (0.670 M) and 2.18 g HEM (0.670 M) as the functional monomers, 3.24 g EGDMA (0.654 M), NIPAM 0.96 g (0.339 M) and 3.24 g TRIM (0.437 M) as cross-linkers, 0.75 g of the "Iniferter" (0.184 M), and 0.18 g PETMP (0.015 M) as a chain transfer agent were dissolved in 25 mL DMF. Then, 0.250 g (0.035 M) of the redox label FcMMA was added to the polymerization mixture, which confers electroactivity to the nanoparticles, as shown in Table S2.

Successively, the polymerization mixture was then degassed using ultrasound and nitrogen bubbling for 15 min in order to remove the oxygen. The amphetamine-functionalised microspheres were used as a solid phase (30 g) and added to the polymerization mixture. The polymerisation was performed by exposure of the mixture (microsphere and the monomer solution) to UV radiation sources (250–450 nm) for 3 min to complete the reaction. Subsequently, the mixture was transferred to a solid phase extraction (SPE) cartridge for the purification process. Afterwards, residues and unreacted monomers were removed from the solid phase by washing with DMF (2 × 100 mL at 4 °C) and ethanol (2 × 100 mL at 4 °C). Following this, the temperature of the SPE cartridge was increased to 70 °C. At this temperature, non-covalent interactions between the template attached to the solid-phase and the high-affinity nanoMIPs were disrupted [37,38]. High affinity MIP nanoparticles were then eluted with ethanol (5 × 20 mL at 70 °C), thus giving pure fractions of particles free of non-specific polymers and residual monomers. For the purification process, 100 mL of nanoMIPs were collected after synthesis and concentrated to 5 mL by evaporation. The nanoparticles were then diluted 10 times in 5 mM PBS and sonicated for 1 min. The resulting nanoMIP solution was recorded as having a concentration of 0.2 mg mL^{-1}. The nanoparticles were then purified using dialysis membranes. For that, the dialysis tube membrane was previously conditioned in water (3 min). Then, nanoMIPs were transferred into the dialysis membrane and confined hermetically with a clip. The membrane was placed in 1 L of distilled water and stirred. The water was changed every 2 h during 8 h and then left overnight, dialysis was monitored using UV–vis spectroscopy. Sodium azide was added to the dialyzed nanoMIP solution at a concentration of 0.02% (w/v) and it was then stored at 4 °C. These nanoMIP particles contain ferrocene units in the polymeric structures, derived from the functionalized monomer used in polymerization process, which confers electroactive properties, resulting in an efficient transducer. Thus, nanoMIPs were further covalently integrated onto electrochemical sensors by drop-casting silanes and by printing using a printer and a composite ink between nanoMIP and graphene.

2.3. Preparation of the sensor using silanes

Screen printed platinum electrodes (SPPE) were activated using a nitrogen plasma cleaner, incubated in a solution that consisted of 6% APTES in ethanol for 1 h. Electrodes were then cured at 130 °C for 30 min. For the immobilization, a suspension of 0.2 mg mL^{-1} nanoMIPs (100 μL) with 52 mmol L^{-1} EDC (0.1 mg mL^{-1}) and 130 mmol L^{-1} NHS (0.15 mg mL^{-1}) dissolved in ethanol was drop-casted on the electrodes surfaces and incubated for two hours. The resulting sensor was rinsed using double distilled water, dried with nitrogen and then stored at 4 ± 0.5 °C and 30% relative humidity.

2.4. Preparation of the sensor using graphene ink

A conductive carbon graphene ink (345 mg, C2171023D1, Sun-Chemical). was mixed with 1 mL of 20% APTES in 1-Methoxy-2-propanol and sonicated for 30 min. The ink was then mixed with 1 mL solution of nanoMIPs (0.1 mg mL^{-1}), 0.4 mg of EDC and 0.6 mg of NHS and vortexed for 15 min. Subsequently, the working electrode from the SPPE was modified by printing with the previously described ink composite. For that, the ink was loaded into cartridges, and then 2 mg of ink per electrode were smoothly deposited using the Voltera PCB Printer (Voltera V One), and then cured for 30 min at 130 °C. The Voltera printer was controlled by V-one Application software (v2.2.0). The printing parameters were previously optimized: nozzle size (255 μm), probe pitch (5 mm), rheological set point (0.16 mm), dispense height (0.10 mm), feed rate (500 mm min^{-1}), pass spacing (0.15 mm), trim length (50 mm), trace penetration (0.15 mm), anti-stringing distance (0.1 mm), kick (0.35 mm), soft start ratio (0.1 mm), and soft step ratio (0.15 mm).

2.5. Electrochemical detection of amphetamine

The electrochemical detection of amphetamine was performed in a concentration range from 75 to 220 nM in a 5 mM PBS (pH 7.4). The same experimental conditions were used to evaluate sensor responses towards other possible interfering compounds, such as dopamine, caffeine, noradrenaline, and paracetamol. The electrochemical responses were investigated by using the previously optimized differential pulse voltammetry (DPV) in the potential range from −0.4 to 0.4 V (vs Ag/AgCl), scan rate of 33 mV s^{-1}, modulation amplitude 200 mV, modulation time at 20 ms and step potential of 50 mV. Lyophilized human plasma powder (S2257–5ML) was reconstituted with 5 mL of 5 mM PBS, mixed and dissolved using a vortex for 3 min, and then centrifuged (3000 g, 5942 rpm). Afterwards, the solution was filtered with a micro-membrane with a syringe filter (25 mm diameter, 0.45 μm PTFE, 87-psi max). Calibration plots were prepared using amphetamine spiked plasma in a concentration range from 75 to 220 nM. Samples (100 μL) were analysed by drop casting on the sensor surface and incubating for 6 min. Then, the DPV measurements were assessed in replicates ($N = 3$). After measuring the voltammetric sensor response, the baseline was corrected, and the blank response was subtracted from the data using the following normalization equation: $\Delta I = \frac{Is-Ib}{Ib}$, where "*ΔI*" represents the *Normalized current*, where "*Is*" indicates sensor response of the sample, and "*Ib*" sensor response for the blank (5 mM PBS or plasma) [46]. Thus, calibration plots were obtained by representing a *Normalized current* (ΔI) against the amphetamine concentration [47–49]. The limit of the detection (LOD) was calculated conventionally from calibration curves using the following equation $LOD=[blank+(3.3 \times STD_{blank})]/slope$, where the blank is the measurement at zero concentration of the analyte and the STD is the standard deviation [50–53].

2.6. Characterization of nanoparticles

Dynamic light scattering (DLS) was employed to measure the hydrodynamic diameter of the particles using a Zetasizer Nano (Nano-S) from Malvern Instruments Ltd. (Malvern, UK). For these measurements, 1 mL solution of nanoparticles was previously sonicated for 1 min to disrupt potential agglomerates. For the polymer characterisation, transmission electron microscopy (TEM) images were obtained using a JEOL JEM-1400 TEM equipped with a 120 kV Tungsten Filament and an EMSIS Xarosa 10MP digital camera. The size of the nanoparticles was estimated using ImageJ v. 1.51o software. Polymer colloids were sonicated for 2 min, and then 10 μl of sample were allowed to adsorb for 25 min to a carbon film grid (AGS160 - Agar scientific Ltd). Carbon grids were previously glow discharged in a Quorum Gloqube for 15 s at 20 mA. The elemental analysis and scanning electron microscopy (SEM)

images were captured with an accelerating voltage at 10 kV using a field emission gun (FEG) environmental scanning electron microscope (ESEM) FEI Quanta 650 FEG SEM equipped with energy dispersive x-ray spectrometer and electron backscatter diffraction (EDX). For all samples, the accelerating voltage used was 5 or 10 kV. The chemical structure was confirmed using the infrared spectroscopy analysis performed with a Bruker Alpha platinum- ATR FTIR spectrometer.

The binding and affinity of the nanoMIPs was evaluated using the SPR technique. For this analysis, a Biacore 3000 instrument (GE Healthcare Life Sciences, UK) and gold coated chips (SIA Kit Au, Biacore) were used. Gold coated chips (SIA Kit Au, Biacore) were cleaned using a helium plasma treatment (RF, 13.56 MHz, EMITECH K1050X). Firstly, gold chips were washed with ethanol, and then functionalized with amino groups by incubating overnight in a solution 0.2 mg mL^{-1} of cysteamine in ethanol. These chips were functionalized with nanoMIPs (0.2 mg mL^{-1}), via immobilization through a carbodiimide chemical reaction with 52 mM EDC (0.1 mg mL^{-1}) and 130 mM NHS (0.15 mg mL^{-1}) dissolved in water. SPR analysis was performed by measuring the binding response between the nanoMIP modified gold chip and a series of analyte injections at different concentrations. All experiments were performed at 25 °C using 5 mM PBS, pH 7.4 as a running buffer at a flow rate 25 μL min^{-1} for analyte injections. For the analytes, 100 μL aliquots of the standard solutions (amphetamine) were injected in the concentration range of 0.01–5 nM. The sensor response and dissociation were analysed for 6 min after the injection using the KINJECT mode. Afterwards, the kinetic data was fitted using BIA evaluation Software v.4.1 (Biacore, GE Heathcare, UK). SPR experimental conditions and fitting were followed as previous optimizations [39,54,55].

3. Results and discussion

3.1. Characterization of nanoparticles

The hydrodynamic particle diameter measured by DLS was found to be 143±38 nm. Similarly, TEM measurements for nanoMIP shown discrete homogeneous spherical particles with a size at 142±22 nm, no aggregates were observed as shown in Fig. 2. The polydispersity index (PDI) was found at 0.157, indicating that the particles are homogenous. The yield obtained per 30 g of glass microspheres was 6 mg of nanoMIPs.

SEM analysis and EDX mapping were additionally performed to characterise the modified SPPE with nanoMIP/graphene, as shown in Fig. 3. The modified electrodes presented a granular and high surface area. The EDX analysis display the presence of C (K_α at 0.277 keV), Fe (K_α at 6.398 keV and L_α at 0.705 keV) and Si (K_α at 1.739 keV), confirming the presence of the graphene, silanes and nanoMIPs including the ferrocene redox probe as shown in Fig. S3. The control SPPE/graphene shown flake-like and smoother surface, characteristic from the graphene (Fig. S4). The EDX analysis displayed the characteristic C (K_α at 0.277 keV) signal and the Pt (L_α at 9.441 keV and M at 2.048 keV). Additionally, the control SPPE bare electrodes present a porous granular surface and the EDX mapping shows only the Pt (L_α at 9.441 keV and M at 2.048 keV) signals (Fig. S5). These results confirm the attachment of the nanoMIPs to the SPPE.

3.2. NanoMIP affinity using SPR

The amphetamine-imprinted nanoMIPs was evaluated using SPR analysis. The nanoMIPs were immobilised on the SPR chip and the interaction was measured against a series of amphetamine injections with different concentrations from 0.01 to 0.25 nM (Fig. S6). The dissociation constants (Kd) for amphetamine on the sensor surface with immobilized nanoMIPs were calculated using BiaEvaluation software v4.1 with 1:1 Langmuir binding model fitting after subtraction of drift and bulk components. The Kd of the interaction of the amphetamine with amphetamine specific nanoMIPs has been estimated as 3.61 nM (Chi2 = 0.31). The fitting confidence value was Chi^2 at 16.9 RU with a maximal response (Rmax) at 236 RU. Chi^2 obtained is less than 10% of Rmax, which means a good fit between the theoretical binding model and the experimental data.

3.3. Optimisation of sensor printing

The nanoMIP sensor preparation by drop casting using silanes was previously optimized [32,56]. In this work, a new 3D printing approach using graphene ink was employed to immobilise nanoMIPs on SPPE. This approach was optimized by varying the amount of graphene ink employed. Sensors were printed using different graphene to nanoMIPs ratios, and then compared to the control sensor (naked graphene printed

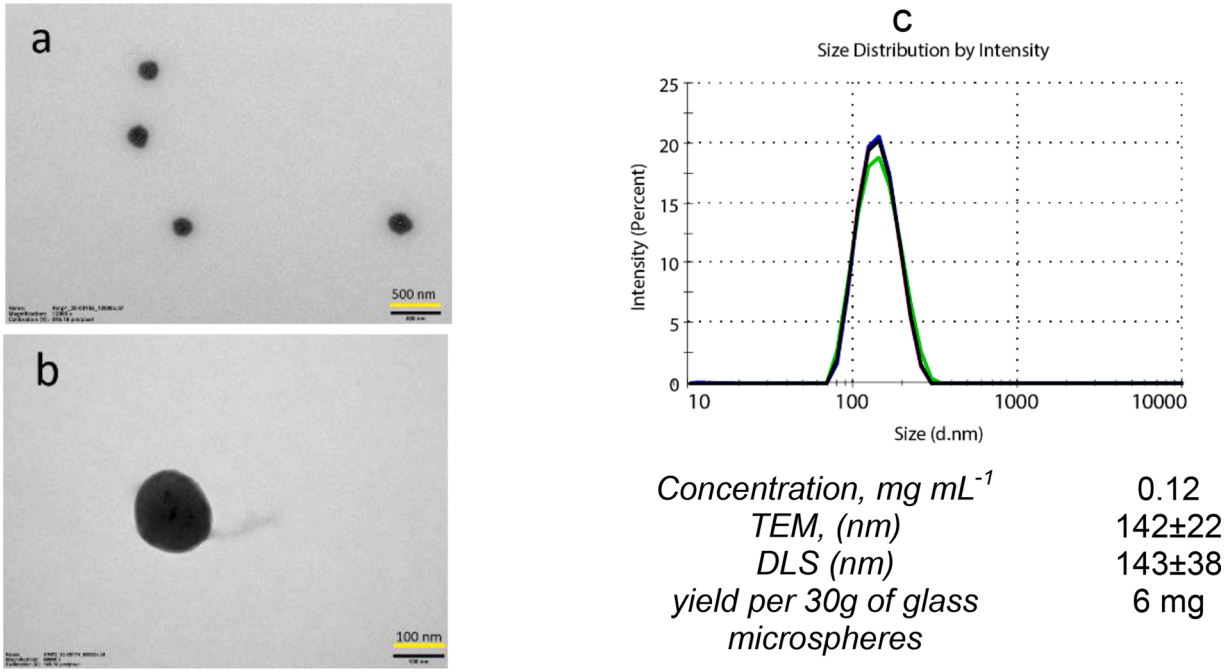

Fig. 2. TEM images for nanoMIPs specific for amphetamine with a scale bar at (a) 500 nm and (b) 100 nm. (c) DLS results for nanoMIPs specific to amphetamine.

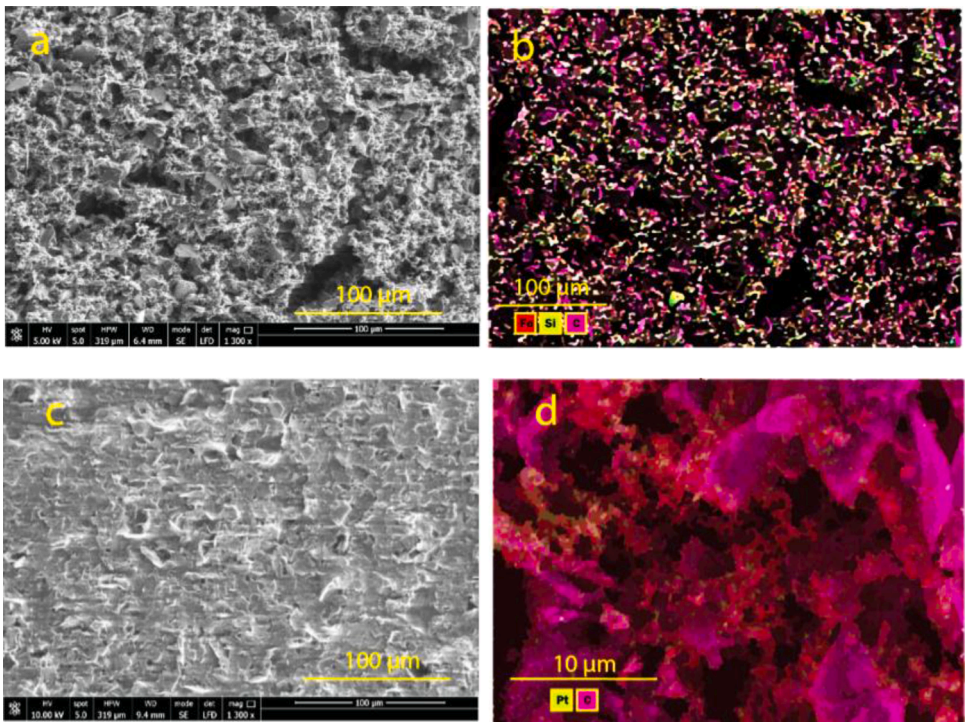

Fig. 3. SEM and EDX elemental analysis mapping for iron, silicon and carbon at 100 µm for (a-b) nanoMIPs deposited on SPPE and (c-b) control carbon ink deposited on bare SPPE at 100 and 10 µm.

on SPPE). In addition, a comparison against sensors prepared using nanoMIPs alone (with silane immobilization) was performed. For this, the graphene to nanoMIP mass ratio was varied from 120 to 85,500 by keeping the nanoMIP mass constant (0.1 mg). The sensor response was evaluated by comparing the calibration curves against amphetamine (75 to 220 nM) as shown in Fig. S7, Supporting information. The combination of graphene and nanoMIPs resulted in a composite that increased the sensitivity 5-fold compared to the nanoMIPs alone. In addition, the composite layer is deposited on the electrode surface by 3D printing. The optimal graphene to nanoMIP mass ratio was found at 3450 (Fig. S7). It was observed that higher concentrations of graphene decrease the sensor signal. The sensor controls printed in the absence of nanoMIPs, and only graphene does not show any response. The main advantage of this 3D printing approach is the straightforward manufacturing process and increased performance and stability.

3.4. Principle of the sensor operation

NanoMIPs contain a ferrocene monomer in the polymeric structures, which confers electroactive properties, resulting in an efficient transducer. The present nanoMIP sensor technology combines recognition and signalling properties, allowing direct electron communication between the nanoparticle binding site and the electrode [19]. The sensor response relies on the nanoMIPs actuation as a result of the recognition of the analyte. This actuation mechanism is known as “Induced fit“ in enzymes [57,58]. The analyte recognition triggers the nanoMIPs conformational changes. As a result, the ferrocene electroactive moieties are exposed, increasing the electron transfer rate. Therefore, the actuation is highly selective, and the analyte concentration is directly related to the change in the current response of the sensor [19]. The nanoMIPs display the characteristic ferrocene electrochemical signal, which can be monitored as a redox marker during electrochemical determinations. This nanoMIPs mechanism is effective for both approaches, the nanoMIPs alone and nanoMIP/graphene-based sensors.

3.5. Electrochemical performance of the nanoMIP/silane sensors

The response of the nanoMIP sensor without graphene increased in direct proportion to the amphetamine concentration (Fig. S8). The analysis was performed as shown in Section 2.5. To consider the sensor variability and allow an accurate comparison is necessary to calculate the *Normalized current*. Thus, the calibration plots display the sensor’s " *Normalized current* " calculated by the blank extraction and the baseline correction. In that way, results from different sensors and matrixes can be compared. The nanoMIP redox signal from the ferrocene was observed at 15 mV (vs Ag/AgCl) in amphetamine spiked solutions in 5 mM PBS in a concentration range from 75 to 220 nM. The nanoMIP/silane sensor presented a sensitivity at 0.133 µA nM^{-1} (R^2=0.999) and LOD at 56 nM (RSD, 3.5%). Similarly, the same sensor was tested on spiked human plasma. In this case, the redox ferrocene signal was observed at 50 mV vs Ag/AgCl. The sensor response presented a sensitivity at 0.128 µA nM^{-1} (R^2=0.996) and LOD at 64 nM (RSD, 3.3%) as shown in Fig. S8. Thus, the plasma influenced the polymer sensor response and sensitivity, the matrix effect was found at 3.7%.

3.6. Electrochemical responses of the nanoMIP/graphene sensors

After printing nanoMIP/graphene sensors, they were directly used without any pre-treatment. DPV measurements display the characteristic oxidation current response related to the electroactivity of nanoMIPs, as conferred by the ferrocene moieties in the polymer structure. The current signal was directly proportional to the amphetamine concentration. The sensor displayed a sensitivity of 0.103 µA nM^{-1} (R^2=0.997) and LOD at 62 nM (RSD, 3.6%) towards amphetamine spiked solutions prepared in 5 mM PBS in a concentration range from 75 to 220 nM as shown in Fig. 4. The nanoMIP/graphene potential was not affected for amphetamine spiked solutions in human plasma and buffer solutions, which was observed at 15 mV (vs Ag/AgCl) in both cases. The sensitivity of the sensor was found at 0.073 µA nM^{-1} (R^2 = 0.995) and LOD at 68 nM (RSD, 2.4%). In this case, it was observed that plasma influenced on the polymer sensitivity having a matrix effect of 29%. The

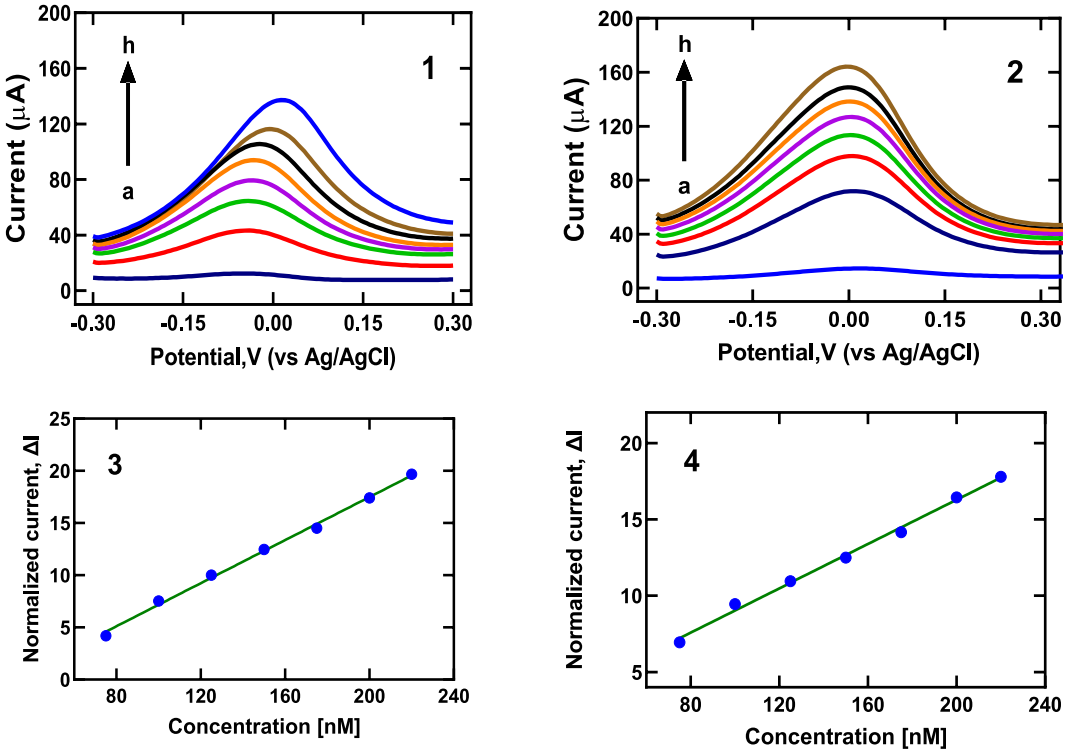

Fig. 4. DPV response of printed nanoMIP/graphene sensor to amphetamine solutions in spiked (1) 5 mM PBS and (2) human plasma in a concentration range of (a) 0, (b) 75, (c) 100, (d) 125, (e) 150, (f) 175, (g) 200 and (h) 220 nM. Resulting sensor calibration plot in spiked (3) 5 mM PBS and (4) plasma, from DPV values with blank subtracted and baseline corrected.

nanoMIP/silane sensor displayed 21.2% higher sensitivity towards amphetamine than nanoMIP/graphene sensor. The increase in the sensitivity using nanoMIP/silane might be due to the greater exposure of the nanoparticles to the target analyte. Whereas in the graphene ink, the nanoMIPs are less accessible for the recognition process. Additionally, control experiment was performed by measuring the DPV response of nanoMIP prepared with no ferrocene and compared against nanoMIP/silane and nanoMIP/graphene. As shown in Fig. **S9**, only sensor prepared with ferrocene presented a signal to 220 nM Amphetamine standard, no signal was observed for nanoMIP with no ferrocene.

3.7. Selectivity and stability of the sensor

The nanoMIP/silane and nanoMIP/graphene sensors were tested against potential biological interferences. Sensor responses to exogenous (caffeine, paracetamol, and cathinone) and endogenous interferences (noradrenaline and dopamine) were recorded and compared to amphetamine response in the same concentration range (75–220 nM), as shown in Fig. 5. The nanoMIP/silane sensor does not show significant interference from caffeine (18%), dopamine (0.2%), noradrenaline (0.5%), paracetamol (23.2%) or cathinone (17%) as shown in Table S3. The non-specific interaction related to Paracetamol and Caffeine is mainly due to functional groups, and smaller molecular size allowing them to interact with the polymer cavity. This interference can be avoided by using a current cut-off at 9.5 μA; as a result, the linear working range is adjusted to 100–220 nM, as shown in Fig. 5.

The nanoMIP/graphene sensor shown no significant interference from caffeine (11.3%), dopamine (0.1%), noradrenaline (0.3%), paracetamol (7%) or cathinone (4.4%) as shown in Table S4. The nanoMIP/graphene sensor presents higher specificity and considerably lower interaction towards paracetamol, cathinone and caffeine. Therefore, the sensor response to interferences was negligible, non-specific and not linear. Potential interference was reduced by implementing a cut-off at 6.5 μA and adjusting the linear range from 100 to 220 nM, as shown in

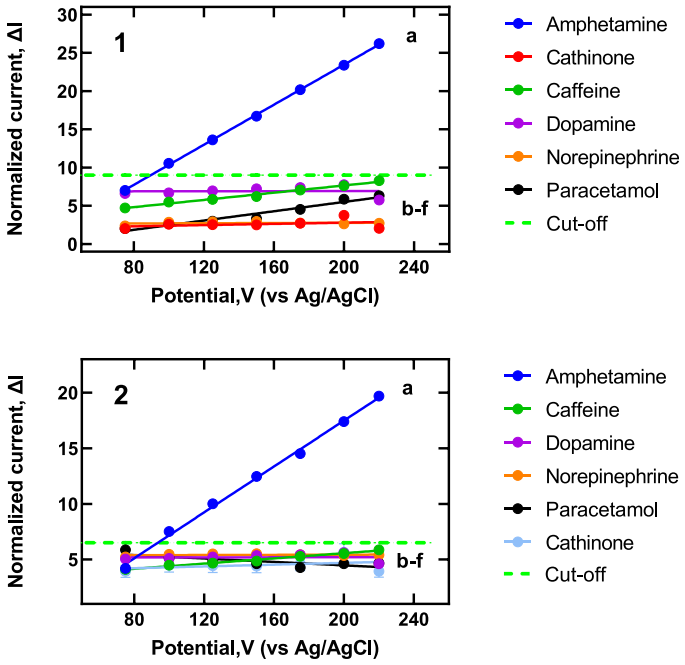

Fig. 5. Selectivity studies for (1) nanoMIP/silane prepared by drop casting and (2) nanoMIP/graphene sensor prepared by printing nanoMIP-graphene on SPPE. The Calibration plots show the response to (a) amphetamine, (b) paracetamol, (c) caffeine, (d) dopamine, (e) noradrenaline and (f) cathinone in a concentration range from 75 up to 220 nM in 5 mM PBS (pH 7.4).For the DPV values, blank was subtracted and baseline corrected.

Fig. 5. The results indicate a higher amphetamine selectivity in the nanoMIP/graphene sensor relative to the nanoMIP/silane sensors. The lower selectivity of the nanoMIP/silane sensor may result from the drop-casting preparation and use of silanes. This method could lead to polymer nanoparticle aggregation, leading to non-specific binding. While in the nanoMIP/graphene printed sensor, the graphene carrier facilitates nanoparticle dispersion, leading to higher recognition. The graphene also increases the conductivity and charge transfer. Therefore, higher responses and selectivity are obtained.

The stability and shelf life of the sensors were assessed by evaluating their performance over time. Both sensors were prepared under similar conditions and then stored in a chamber at 22 °C and 60% humidity for 122 days. Sensors were tested independently for a period ranging from one to 112 days, nine electrodes per deposition method. The sensor current response to an amphetamine standard solution (200 nM) was tested, and the sensor stability obtained is summarized in Fig. S10. Herein, the average response and standard deviation are displayed every 14 days. According to these results, after 28 days, the NanoMIP/graphene response was 99.4%, and the nanoMIP/silane was 98.3%, presenting similar performance. After 56 days, the sensor response fell 9.8% and 14.2% for the nanoMIP/graphene and nanoMIP/silane sensors, respectively. These results comply with industrial standards [59–61]. The sensors remained functional until 112 days, at which time the overall decrease in the sensor response was 20.2% and 27.5% for the nanoMIP/graphene sensor and nanoMIP/silane sensor, correspondingly. Therefore, after this period, sensor readings required adjustment. For that, a storage factor can be used to obtain the equivalent corrected response. Future work will focus on improving the storage conditions by keeping the sensors in dry conditions. The nanoMIP/graphene sensor performance was evaluated by measuring the repeatability, reproducibility, and stability. The repeatability was assessed by measuring the sensor response five times to amphetamine standard (200 nM) in a single sensor and under the same conditions by calculating the RSD. The repeatability for a single sensor was 3.6%. The reproducibility was assessed by calculating the RSD of the response for ten different sensors to an amphetamine standard (200 nM) under identical conditions and was found to be 5.4%. The previous analysis proves that the sensor performance complies with the industrial accuracy standards (ISO-151, 917), which recommends that 95% of the results should be within ± 15% of a laboratory standard [59–61]. Due to the higher selectivity, stability, easy manufacturing and robustness of the nanoMIP/graphene sensor, this platform was selected for the street sample assessment.

3.8. Test on street samples

Stock solution of street powder samples (10 mg) were prepared in water (10 mL) and then diluted accordingly. Afterwards, analysed using UPLC-MS/MS and then measured with the nanoMIP/graphene sensor using the standard addition method (Section 9–10, Supporting information). As a proof of concept, two samples were analysed. The LOD was found at 37.6 nM and RSD at 2.6%. No interference was observed from cutting agents, as shown in Fig. S12. The recoveries were found at 106.5% and 107% for sample 1 and sample 2, respectively, as shown in Table S7.

3.9. Comparison of the analytical performances of the sensor

Several approaches have been used to detect the non-electroactive amphetamine molecule using electrochemical sensors, leading to sensitive and portable devices, as shown in Table 1. Unfortunately, most techniques are not applicable for onsite testing due to their fragility and pre-treatment steps needed, or they are not sufficiently robust to be used for biological and street samples.

For example, the bio-recognition elements used in biosensors limit their application and mass production. In addition, biological receptors are fragile and sensitive to environmental conditions, which might lead to their denaturation, inactivity, and cross-reactivity when tested in biological samples. On the other hand, classical electrochemical sensors use direct electrochemical oxidation of the analyte, leading to potential side reactions, interferences from cutting agents and matrix effects from samples. These parameters affect the accuracy and quantification and might result in signals that are difficult to interpret and false positives results.

Nevertheless, amphetamine cannot be directly determined by electrochemical methods without sample pre-treatment using these traditional methods [68,69]. Several strategies, such as derivatization or sample pre-treatment, are helpful for lab base testing but not practical for field applications, which allow only qualitative determinations. Alternatively, generic macrocycles and polymers have been used to determine amphetamine using impedance, capacitance, and field-effect transistors [64–66]. These are unsuitable for on-field applications due to the lack of selectivity and matrix effect. The present technology overcomes all these challenges and allows direct and accurate quantification of amphetamine in human plasma and street samples. In addition, printed sensors lead to a reproducible and cost-effective technique and, when used with portable sensor devices, could help in drug screening, and point of care diagnostics.

4. Conclusion

Electroactive molecularly imprinted polymer nanoparticles (nanoMIP) were designed by molecular modelling. First, the Sybyl package was Electroactive molecularly imprinted polymer nanoparticles (nanoMIP) were designed by molecular modelling. Sybyl package was successfully used to select the most appropriate functional monomers (ITA and HEM). Then, MOE packages confirm that both monomers interact strongly with the amphetamine leading to a recognition pocket. The nanoMIP were obtained successfully using solid phase synthesis, resulting in discrete spherical particles with a diameter of 142±22 nm. The SPR sensorgrams confirm the interaction between the nanoMIP and the amphetamine, leading to strong interaction (Kd of 3.61 nM).

Two approaches were engineered to integrate nanoMIP on

Table 1
Amphetamine sensor techniques available and their performance.

Recognition unit	Analysed sample	Detection method	LOD	Linear range	Refs.
Aptasensor	Urine water	Voltammetry	0.51 nM	0.1–1.0 nM	[62]
Immunosensor	Urine	Amperometry	2.5 μM	0.74 −14.8 mM	[63]
Cucurbit[7]uril	Urine	Field-effect transistors	1 nM	1 nM-1 μM	[64]
AuNPs@ cucurbit[7]uril	Urine Plasma	Impedance	6.2 pM	10 pM-100 μM	[65]
PVC/plasticizers/ionophore (dibenzo-18-crown 6-ether)	Buffer	Potentiometric	0.4 μM	0.1μM-1mM	[66]
MIP, Poly-tyramine	Sewage and tap water	Capacitance	50 μM	NR	[67]
Electrochemical oxidation by *in situ* derivatization	Street samples	Voltammetry	22.2 μM	50–500 μM	[68]
Electrochemical oxidation by *in situ* derivatization	Street samples	Voltammetry	0.3 mM	0.50–1.25 mM	[69]
$[Ru(bpy)_3]^{2+}$ Nafion composite	Milli-Q water	Electro-chemiluminescence	50 pM	50 pM-1 mM	[70]
NanoMIP/graphene	Buffer	Voltammetry	62 nM	75–220 nM	This work
NanoMIP/graphene	Plasma	Voltammetry	68 nM	75–220 nM	
NanoMIP/graphene	Street samples	Voltammetry	37.6 nM	25–220nM	

electrodes. Firstly, the particles were covalently attached using carbodiimide chemistry and silanes by drop-casting. Alternatively, sensors were integrated successfully using a graphene composite and 3D printing technology. The ink composition was optimized by tuning the proportion of nanoMIP in the graphene composite, and the 3D printing parameters were adjusted correspondingly. It was observed that the use of a composite ink based on graphene and nanoMIPs resulted in obtaining a better signal for the detection of amphetamine compared to other immobilization methods tested, but also compared to sensors based on mono-component films with graphene or nanoMIPs. In addition, increasing the mass ratio between graphene and nanoMIPs in ink to a maximum value of 3450 determined obtaining a better sensitivity. Additionally, the EDX analysis demonstrated the presence of the ferrocene monomer in the nanoMIP and their integration on electrodes. The nanoMIP/silane sensor presented a LOD 64 nM, sensitivity at 0.128 $\mu A nM^{-1}$(R^2=0.996) and RSD 3.3% in spiked plasma. On the other hand, the nanoMIP-graphene sensors presented at 0.073 $\mu A\ nM^{-1}$ (R^2 = 0.995), LOD at 68 nM with an RSD of 2.4%. The nanoMIP-graphene sensors improve the selectivity, reducing the interference on street samples and biological fluids. In addition, sensor's reproducibility and shelf life increased compared to the drop-casting approach.

The sensor allow to detect amphetamine on real street seized samples, these results were validated against UPLC-MS/MS demonstrating satisfactory accuracy and performance for a rapid test that can be used in point-of-care or on field screening services.

The essential advantage of the present sensor technology is that nanoMIP allows high selectivity and avoids the electro-oxidation of interfering molecules due to their actuation system. In addition, the nanoMIP actuation led to a selective molecular recognition system. Unlike classic electrochemical sensors, nanoMIP allows the detection of non-electroactive molecules. In addition, nanoMIP can be easily manufactured using reactors and integrated by 3D printing or screen-printing on a large scale. The present technology reflects the scalability of nanoMIP sensor manufacturing and its potential use in clinical and forensic applications. Future work will focus on improving the sensors' storage, lifetime and working range.

CRediT authorship contribution statement

Meshal H. Almabadi: Investigation, Writing – original draft. **Florina Maria Truta:** Formal analysis, Investigation, Data curation, Writing – review & editing. **Gyako Adamu:** Formal analysis, Investigation, Data curation. **Todd Cowen:** Formal analysis, Investigation, Data curation, Writing – review & editing. **Mihaela Tertis:** Formal analysis, Investigation, Data curation, Writing – review & editing. **Ana-Maria Drăgan:** Formal analysis, Investigation, Data curation, Writing – review & editing. **Kaseb D.M. Alanazi:** Investigation. **Maria-Georgia Ștefan:** Formal analysis, Investigation, Data curation. **Elena Piletska:** Resources, Supervision, Project administration. **Béla Kiss:** Validation, Formal analysis, Investigation, Data curation, Writing – review & editing. **Cecilia Cristea:** Writing – review & editing, Resources, Supervision, Project administration, Funding acquisition. **Karolien De Wael:** Project administration, Funding acquisition. **Sergey A. Piletsky:** Resources, Supervision, Project administration, Funding acquisition. **Alvaro Garcia Cruz:** Conceptualization, Methodology, Validation, Formal analysis, Investigation, Data curation, Writing – original draft, Writing – review & editing, Supervision, Project administration, Funding acquisition.

Declaration of Competing Interest

The authors declare that they have no known competing financial interests or personal relationships that could have appeared to influence the work reported in this paper.

Data availability

Data will be made available on request.

Acknowledgement

The authors would like to thank the funding from the European project BorderSens (Grant agreement ID: 833787) for the "Border detection of illicit drugs and precursors by highly accurate electro sensors" and the support from the Jeddah University and University of Hail (Saudi Arabia). Furthermore, the authors are thankful for the help of the General Inspectorate of Romanian Police (IGPR) and Crime Brigade (BCCO) from Cluj-Napoca who kindly provided street samples.

Supplementary materials

Supplementary material associated with this article can be found, in the online version, at doi:10.1016/j.electacta.2023.142009.

References

[1] X. Castells, L. Blanco-Silvente, R. Cunill, Amphetamines for attention deficit hyperactivity disorder (ADHD) in adults, Cochrane Database Syst. Rev. (2018).
[2] J. Shakeri, S.M. Ahmadi, F. Maleki, M.R. Hesami, A.P. Moghadam, A. Ahmadzade, M. Shirzadi, A. Elahi, Effectiveness of group narrative therapy on depression, quality of life, and anxiety in people with amphetamine addiction: a randomized clinical trial, Iran. J. Med. Sci. 45 (2020) 91.
[3] V.C. Abad, C. Guilleminault, New developments in the management of narcolepsy, Nat. Sci. Sleep 9 (2017) 39.
[4] J. Harro, Neuropsychiatric adverse effects of amphetamine and methamphetamine, Int. Rev. Neurobiol. 120 (2015) 179–204.
[5] D.M. Stoneberg, R.K Shukla, M.B. Magness, Global methamphetamine trends: an evolving problem, Int. Crim. Justice Rev. 28 (2) (2018) 136–161.
[6] H. Gjerde, A.S. Christophersen, B. Skuterud, K. Klemetsen, J. Mørland, Screening for drugs in forensic blood samples using EMIT® urine assays, Forensic Sci. Int. 44 (1990) 179–185.
[7] H. Gjerde, I. Hasvold, G. Pettersen, A.S. Christophersen, Determination of amphetamine and methamphetamine in blood by derivatization with perfluorooctanoyl chloride and gas chromatography/mass spectrometry, J. Anal. Toxicol. 17 (1993) 65–68.
[8] I. Gustavsen, J. Mørland, J.G. Bramness, Impairment related to blood amphetamine and/or methamphetamine concentrations in suspected drugged drivers, Accident Anal. Prevention 38 (2006) 490–495.
[9] M. Philp, S. Fu, A review of chemical 'spot'tests: a presumptive illicit drug identification technique, Drug Test. Anal. 10 (2018) 95–108.
[10] F. Coppey, A. Bécue, P.Y. Sacré, E.M. Ziemons, P. Hubert, P. Esseiva, Providing illicit drugs results in five seconds using ultra-portable NIR technology: an opportunity for forensic laboratories to cope with the trend toward the decentralization of forensic capabilities, Forensic Sci. Int. 317 (2020), 110498.
[11] C. Weyermann, Y. Mimoune, F. Anglada, G. Massonnet, P. Esseiva, P. Buzzini, Applications of a transportable Raman spectrometer for the *in situ* detection of controlled substances at border controls, Forensic Sci. Int. 209 (2011) 21–28.
[12] Z. Du, T. Sun, J. Zhao, D. Wang, Z. Zhang, W. Yu, Development of a plug-type IMS-MS instrument and its applications in resolving problems existing in *in-situ* detection of illicit drugs and explosives by IMS, Talanta 184 (2018) 65–72.
[13] L. Harper, J. Powell, E.M. Pijl, An overview of forensic drug testing methods and their suitability for harm reduction point-of-care services, Harm Reduct. J. 14 (1) (2017) 1–13.
[14] A.M. Dragan, M. Parrilla, B. Feier, R. Oprean, C. Cristea, K. De Wael, Analytical techniques for the detection of amphetamine-type substances in different matrices: a comprehensive review, TrAC Trends Anal. Chem. 145 (2021), 116447.
[15] E. Garrido, J. Garrido, N. Milhazes, F. Borges, A. Oliveira-Brett, Electrochemical oxidation of amphetamine-like drugs and application to electroanalysis of ecstasy in human serum, Bioelectrochemistry 79 (2010) 77–83.
[16] A. Florea, M. de Jong, K. De Wael, Electrochemical strategies for the detection of forensic drugs, Curr. Opin. Electrochem. 11 (2018) 34–40.
[17] O.S. Ahmad, T.S. Bedwell, C. Esen, A. Garcia-Cruz, S.A. Piletsky, Molecularly imprinted polymers in electrochemical and optical sensors, Trends Biotechnol. 37 (2019) 294–309.
[18] M. Dronova, E. Smolianitski, O. Lev, Electrooxidation of new synthetic cannabinoids: voltammetric determination of drugs in seized street samples and artificial saliva, Anal. Chem. 88 (2016) 4487–4494.
[19] A. Garcia-Cruz, O. Ahmad, K. Alanazi, E. Piletska, S. Piletsky, Generic sensor platform based on electro-responsive molecularly imprinted polymer nanoparticles (e-NanoMIPs), Microsyst. Nanoeng. 6 (2020) 1–9.
[20] E. De Rycke, C. Stove, P. Dubruel, S. De Saeger, N. Beloglazova, Recent developments in electrochemical detection of illicit drugs in diverse matrices, Biosens. Bioelectron. (2020), 112579.

[21] L. Shaw, L. Dennany, Applications of electrochemical sensors: forensic drug analysis, Curr. Opin. Electrochem. 3 (2017) 23–28.
[22] F.W. Scheller, X. Zhang, A. Yarman, U. Wollenberger, R.E. Gyurcsányi, Molecularly imprinted polymer-based electrochemical sensors for biopolymers, Curr. Opin. Electrochem. 14 (2019) 53–59.
[23] A. Adumitrăchioaie, M. Tertiș, A. Cernat, R. Săndulescu, C. Cristea, Electrochemical methods based on molecularly imprinted polymers for drug detection. A review, Int. J. Electrochem. Sci 13 (2018) 2556–2576.
[24] Z. Stojanovic, J. Erdőssy, K. Keltai, F.W. Scheller, R.E. Gyurcsányi, Electrosynthesized molecularly imprinted polyscopoletin nanofilms for human serum albumin detection, Anal. Chim. Acta 977 (2017) 1–9.
[25] A.G. Ayankojo, J. Reut, V. Ciocan, A. Öpik, V. Syritski, Molecularly imprinted polymer-based sensor for electrochemical detection of erythromycin, Talanta 209 (2020), 120502.
[26] P.S. Sharma, A. Garcia-Cruz, M. Cieplak, K.R. Noworyta, W. Kutner, Gate effect'in molecularly imprinted polymers: the current state of understanding, Curr. Opin. Electrochem. 16 (2019) 50–56.
[27] V.M. Ekomo, C. Branger, R. Bikanga, A.M. Florea, G. Istamboulie, C. Calas-Blanchard, T. Noguer, A. Sarbu, H. Brisset, Detection of Bisphenol A in aqueous medium by screen printed carbon electrodes incorporating electrochemical molecularly imprinted polymers, Biosens. Bioelectron. 112 (2018) 156–161.
[28] D. Udomsap, C. Branger, G. Culioli, P. Dollet, H. Brisset, A versatile electrochemical sensing receptor based on a molecularly imprinted polymer, Chem. Commun. 50 (2014) 7488–7491.
[29] T. Alizadeh, M. Akhoundian, M.R. Ganjali, A ferrocene/imprinted polymer nanomaterial-modified carbon paste electrode as a new generation of gate effect-based voltammetric sensor, New J. Chem. 42 (2018) 4719–4727.
[30] A. Motaharian, K. Naseri, O. Mehrpour, S. Shoeibi, Electrochemical determination of atypical antipsychotic drug quetiapine using nano-molecularly imprinted polymer modified carbon paste electrode, Anal. Chim. Acta 1097 (2020) 214–221.
[31] S. Khumngern, P. Thavarungkul, P. Kanatharana, T. Bejrananda, A. Numnuam, Molecularly imprinted electrochemical sensor based on poly (o-phenylenediamine-co-o-aminophenol) incorporated with poly (styrenesulfonate) doped poly (3, 4-ethylenedioxythiophene) ferrocene composite modified screen-printed carbon electrode for highly sensitive and selective detection of prostate cancer biomarker, Microchem. J. 177 (2022), 107311.
[32] A. Fatoni, A. Numnuam, P. Kanatharana, W. Limbut, P. Thavarungkul, A novel molecularly imprinted chitosan–acrylamide, graphene, ferrocene composite cryogel biosensor used to detect microalbumin, Analyst 139 (2014) 6160–6167.
[33] A. Poma, A. Guerreiro, S. Caygill, E. Moczko, S. Piletsky, Automatic reactor for solid-phase synthesis of molecularly imprinted polymeric nanoparticles (MIP NPs) in water, RSC Adv. 4 (2014) 4203–4206.
[34] A. Yarman, F.W. Scheller, How reliable is the electrochemical readout of MIP sensors? Sensors 20 (2020) 2677.
[35] S.A. Piletsky, A.P. Turner, Electrochemical sensors based on molecularly imprinted polymers, Electroanalysis An Int. J. Devoted Fund. Pract. Asp. Electroanal. 14 (2002) 317–323.
[36] A. Garcia-Cruz, T. Cowen, A. Voorhaar, E. Piletska, S.A. Piletsky, Molecularly imprinted nanoparticles-based assay (MINA)–detection of leukotrienes and insulin, Analyst 145 (2020) 4224–4232.
[37] A.G. Cruz, I. Haq, T. Cowen, S. Di Masi, S. Trivedi, K. Alanazi, E. Piletska, A. Mujahid, S.A. Piletsky, Design and fabrication of a smart sensor using *in silico* epitope mapping and electro-responsive imprinted polymer nanoparticles for determination of insulin levels in human plasma, Biosens. Bioelectron. 169 (2020), 112536.
[38] I. Haq, K.D. Alanazi, J. Czulak, S. Di Masi, E. Piletska, A. Mujahid, T. Hussain, S. Piletsky, A.G. Cruz, Determination of sitagliptin in human plasma using a smart electrochemical sensor based on electroactive molecularly imprinted nanoparticles, Nanoscale Adv. (2021).
[39] K. Alanazi, A.G. Cruz, S. Di Masi, A. Voorhaar, O.S. Ahmad, T. Cowen, E. Piletska, N. Langford, T.J. Coats, M.R. Sims, Disposable paracetamol sensor based on electroactive molecularly imprinted polymer nanoparticles for plasma monitoring, Sens. Actuators B 329 (2021), 129128.
[40] H. Munawar, K. Smolinska-Kempisty, A.G. Cruz, F. Canfarotta, E. Piletska, K. Karim, S.A. Piletsky, Molecularly imprinted polymer nanoparticle-based assay (MINA): application for fumonisin B1 determination, Analyst 143 (2018) 3481–3488.
[41] D. López-Puertollano, T. Cowen, Á. García-Cruz, E. Piletska, A. Abad-Somovilla, A. Abad-Fuentes, S. Piletsky, Study of epitope imprinting for small templates: preparation of nanoMIPs for ochratoxin A, ChemNanoMat 5 (2019) 651–657.
[42] A. Herrera-Chacón, X. Cetó, M. Del Valle, Molecularly imprinted polymers-towards electrochemical sensors and electronic tongues, Anal. Bioanal. Chem. 413 (2021) 6117–6140.
[43] E. Mazzotta, A. Turco, I. Chianella, A. Guerreiro, S.A. Piletsky, C. Malitesta, Solid-phase synthesis of electroactive nanoparticles of molecularly imprinted polymers. A novel platform for indirect electrochemical sensing applications, Sens. Actuators B 229 (2016) 174–180.
[44] K. Smolinska-Kempisty, O.S. Ahmad, A. Guerreiro, K. Karim, E. Piletska, S. Piletsky, New potentiometric sensor based on molecularly imprinted nanoparticles for cocaine detection, Biosens. Bioelectron. 96 (2017) 49–54.
[45] R. D'Aurelio, I. Chianella, J.A. Goode, I.E. Tothill, Molecularly imprinted nanoparticles based sensor for cocaine detection, Biosensors 10 (2020) 22.
[46] M.D. Peris-Díaz, A. Krężel, A guide to good practice in chemometric methods for vibrational spectroscopy, electrochemistry, and hyphenated mass spectrometry, TrAC Trends Anal. Chem. 135 (2021), 116157.
[47] R.B. Clark, J.E. Dick, Electrochemical sensing of perfluorooctanesulfonate (PFOS) using ambient oxygen in river water, ACS Sens. 5 (2020) 3591–3598.
[48] D.A. Bernards, D.J. Macaya, M. Nikolou, J.A. DeFranco, S. Takamatsu, G. G. Malliaras, Enzymatic sensing with organic electrochemical transistors, J. Mater. Chem. 18 (2008) 116–120.
[49] M.A. Tabrizi, J.P. Fernández-Blázquez, D.M. Medina, P. Acedo, An ultrasensitive molecularly imprinted polymer-based electrochemical sensor for the determination of SARS-CoV-2-RBD by using macroporous gold screen-printed electrode, Biosens. Bioelectron. 196 (2022), 113729.
[50] D.A. Armbruster, T. Pry, Limit of blank, limit of detection and limit of quantitation, Clin. Biochem. Rev. 29 (2008) S49.
[51] S.K. Vashist, J.H. Luong, Bioanalytical requirements and regulatory guidelines for immunoassays, Handb. Immunoassay Technol. (2018) 81–95. Elsevier.
[52] A.S. Lister, Validation of HPLC methods in pharmaceutical analysis, Sep. Sci. Technol. (2005) 191–217. Elsevier.
[53] O. González, R.M. Alonso, Validation of bioanalytical chromatographic methods for the quantification of drugs in biological fluids, Handb. Analytical Separ. (2020) 115–134. Elsevier.
[54] J. Mistry, A. Guerreiro, E. Moczko, E. Piletska, K. Karim, S.A. Piletsky, Analysis of cooperative interactions in molecularly imprinted polymer nanoparticles, Mole. Imprinting 3 (2015) 55–64.
[55] B. Abbott, T.S. Bedwell, F. Grillo, S. Piletsky, M.J. Whitcombe, E. Piletska, A. Garcia-Cruz, T. Cowen, S.A. Piletsky, Use of polymeric solid phase in synthesis of MIP nanoparticles for biotin, React. Funct. Polym. 170 (2022), 105109.
[56] I. Haq, K. Alanazi, J. Czulak, S. Di Masi, E. Piletska, A. Mujahid, T. Hussain, S. A. Piletsky, A. Garcia-Cruz, Determination of sitagliptin in human plasma using a smart electrochemical sensor based on electroactive molecularly imprinted nanoparticles, Nanoscale Adv. 3 (2021) 4276–4285.
[57] F. Paul, T.R. Weikl, How to distinguish conformational selection and induced fit based on chemical relaxation rates, PLoS Comput. Biol. 12 (2016), e1005067.
[58] A.D. Vogt, E. Di Cera, Conformational selection or induced fit? A critical appraisal of the kinetic mechanism, Biochemistry 51 (2012) 5894–5902.
[59] I.O.f. Standardization, *In vitro* Diagnostic Test systems: Requirements For Blood-Glucose Monitoring Systems For Self-Testing in Managing Diabetes Mellitus, ISO, 2003.
[60] A. Baumstark, S. Pleus, C. Schmid, M. Link, C. Haug, G. Freckmann, Lot-to-lot variability of test strips and accuracy assessment of systems for self-monitoring of blood glucose according to ISO 15197, J. Diabetes Sci. Technol. 6 (2012) 1076–1086.
[61] G. Freckmann, C. Schmid, A. Baumstark, S. Pleus, M. Link, C. Haug, System accuracy evaluation of 43 blood glucose monitoring systems for self-monitoring of blood glucose according to DIN EN ISO 15197, J. Diabetes Sci. Technol. 6 (2012) 1060–1075.
[62] S. Soni, U. Jain, D.H. Burke, N. Chauhan, A label free, signal off electrochemical aptasensor for amphetamine detection, Surf. Interfaces (2022), 102023.
[63] F.M. Ivison, J.W. Kane, J.E. Pearson, J. Kenny, P. Vadgama, Development of a redox mediated amperometric detection system for immunoassay. Application to urinary amphetamine screening, Electroanalysis An Int. J. Devoted Fund. Pract. Asp. Electroanal. 12 (2000) 778–785.
[64] Y. Jang, M. Jang, H. Kim, S.J. Lee, E. Jin, J.Y. Koo, I.C. Hwang, Y. Kim, Y.H. Ko, I. Hwang, Point-of-use detection of amphetamine-type stimulants with host-molecule-functionalized organic transistors, Chem. 3 (2017) 641–651.
[65] H. Li, X. Hu, J. Zhao, K. Koh, H. Chen, A label-free impedimetric sensor for the detection of an amphetamine-type derivative based on cucurbit [7]uril-mediated three-dimensional AuNPs, Electrochem. Commun. 100 (2019) 126–133.
[66] J. Gallardo-González, A. Baraket, A. Bonhomme, N. Zine, M. Sigaud, J. Bausells, A. Errachid, Sensitive potentiometric determination of amphetamine with an all-solid-state micro ion-selective electrode, Anal. Lett. 51 (2018) 348–358.
[67] E. De Rycke, O. Leman, P. Dubruel, M. Hedström, M. Völker, N. Beloglazova, S. De Saeger, Novel multiplex capacitive sensor based on molecularly imprinted polymers: a promising tool for tracing specific amphetamine synthesis markers in sewage water, Biosens. Bioelectron. 178 (2021), 113006.
[68] M. Parrilla, N.F. Montiel, F. Van Durme, K. De Wael, Derivatization of amphetamine to allow its electrochemical detection in illicit drug seizures, Sens. Actuators B 337 (2021), 129819.
[69] J. Schram, M. Parrilla, A. Slosse, F. Van Durme, J. Åberg, K. Björk, S.M. Bijvoets, S. Sap, M.W. Heerschop, K. De Wael, Paraformaldehyde-coated electrochemical sensor for improved on-site detection of amphetamine in street samples, Microchem. J. 179 (2022), 107518.
[70] J. McGeehan, L. Dennany, Electrochemiluminescent detection of methamphetamine and amphetamine, Forensic Sci. Int. 264 (2016) 1–6.